Drug Binding by Branched DNA Molecules: Analysis by Chemical Footprinting of Intercalation into an Immobile Junction†

Qiu Guo, Min Lu, N. C. Seeman, and N. R. Kallenbach*
Department of Chemistry, New York University, New York, New York 10003
Received June 2, 1989; Revised Manuscript Received August 31, 1989

ABSTRACT: Branched DNA structures interact with drugs differently from unbranched control duplexes of similar sequence. A specific interaction between the reagent (methidiumpropyl-EDTA)·Fe(II) [MPE·Fe(II)] and a branched DNA molecule formed from 16-mer oligonucleotide strands has been reported [Guo, Q., Seeman, N. C., & Kallenbach, N. R. (1989) *Biochemistry 28*, 2355–2359]. The structure of the branched molecule is thought to be made up of two double-helical stacking domains with an overall twofold symmetry across the branch site. The MPE-Fe(II) interaction occurs predominantly at or adjacent to the branch site and is eliminated by a second intercalator, propidium iodide. Further studies on the nature and properties of this site are presented here. Comparison of the patterns of scission of linear duplex and branched tetramer by EDTA·Fe(II), MPE·Fe(II), and Cu(I)–(*o*-phenanthroline)$_2$ [(OP)$_2$Cu(I)] provides a higher resolution picture of the site of enhanced binding. In particular, the sensitive footprinting afforded by (OP)$_2$Cu(I) allows us to localize the major site of preferential interaction with propidium precisely to the branch point itself, with a roughly twofold symmetric pattern of cuts resulting. In detail, the differential pattern with respect to each duplex control is distinct for each arm of the junction. Excess propidium results in apparent reversal of the crossover isomer of the junction, indicating a possible additional avenue for the action of drugs in biological systems—effects on the products of recombination.

The site and sequence specificity of the interaction of ligands with DNA are amenable to analysis by means of high-resolution footprinting methods; these procedures are analogous in principle to the Maxam–Gilbert sequencing method (Gilbert et al., 1976; Maxam & Gilbert, 1977). The strategy is to expose end-labeled DNA to a reagent that can induce scission of the polynucleotide backbone, such as an endonuclease, in the absence and presence of ligand (Galas & Schmitz, 1973; Schmitz & Galas, 1979). When the resulting fragments are resolved on denaturing polyacrylamide gels, inhibition or enhancement of cleavage at the site or sites bound by the ligand discloses the corresponding positions of the chain as bands in the gel which show weaker or stronger intensities than are found in uncovered control regions (see Figure 1).

A variety of cleavage reagents have been used successfully as probes in footprinting experiments, including enzymatic nucleases such as DNase I (Galas & Schmitz, 1973), and UV irradiation (Becker & Wang, 1984), as well as a number of chemical species that modify DNA (Ogata & Gilbert, 1977; Siebenlist et al., 1980) or induce radicals in the presence of light or redox agents (Dervan, 1986; Ward et al., 1986; Sigman, 1986; Tullius, 1987). The footprint obtained with a particular reactive probe depends on both the nature of the active species and the mode and strength of interaction between the probe and DNA. The agent MPE·Fe(II) consists of an intercalating ring system covalently tethered to an EDTA moiety which binds iron and can generate OH radicals in the presence of H_2O and peroxide or oxygen (Hertzberg & Dervan, 1982, 1984). Tullius and co-workers have found that EDTA·Fe(II) alone, which does not bind tightly to DNA, provides a sensitive and nonperturbative footprinting reagent for DNA and DNA–protein complexes (Tullius & Dombroski, 1985, 1986). The 2:1 complex of 1,10-phenanthroline with Cu(I), abbreviated here as (OP)$_2$Cu(I) (Sigman, 1986), has been found to have nucleolytic activity via oxidation of deoxyribose (Kuwabara et al., 1987; Goyne & Sigman, 1987) in the presence of oxygen and a reducing agent such as mercaptopropionic acid. This reaction is apparently mediated by binding of the complex to duplex DNA (Marshall et al., 1981), since single-stranded species are not cleaved by this agent (Pope & Sigman, 1984). These reagents are used here as probes of the binding of intercalative drugs to branched DNA.

We have recently reported two studies of the self-footprinting of an "immobile DNA junction", a stable four-armed branched DNA structure, termed J1 (Figure 2), in which branch migration is possible only by breaking Watson–Crick base pairs (Seeman, 1982; Seeman & Kallenbach, 1983; Kallenbach et al., 1983; Seeman et al., 1985). In the first study, it was found that EDTA·Fe(II)-mediated hydroxyl radical cleavage of the junction J1 results in a twofold symmetric cutting pattern on the four strands (Churchill et al., 1988). Two strands exhibit cutting patterns that are similar to those in duplex controls, while the other two show strong protection from cutting at the two bases flanking the branch point. From this result we infer that the four arms are disposed in two helical stacking domains, such that one strand in each domain remains roughly equivalent in conformation to that strand in an intact duplex, while the second strand crosses over from one stack to the other (Figure 2). This is in agreement with gel electrophoresis experiments conducted by Cooper and Hagerman (1987), Duckett et al. (1988), and ourselves (Seeman et al., 1989); these experiments are consistent with the preferred orientation of the junction being that illustrated on the left, with the two non-crossover strands roughly antiparallel. The second study (Chen et al., 1988) shows that the distribution of double-helical arms into the two helical domains is a function of the sequence that flanks the branch point, an observation also confirmed by electrophoretic studies (Duckett et al., 1988).

† This research was supported by Grants CA-24101 and GM-29554 from the National Institutes of Health.
* Author to whom correspondence should be addressed.

0006-2960/90/0429-570$02.50/0

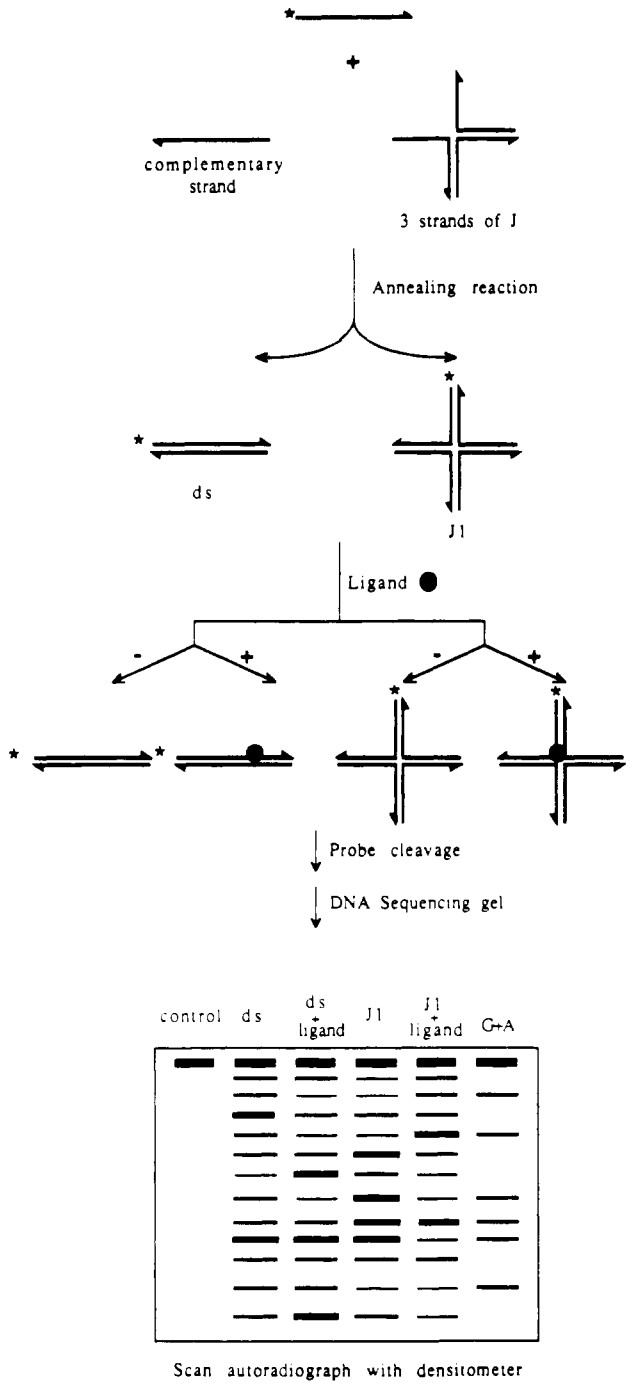

FIGURE 1: Strategy of the experiments in this study. Each strand of the tetramer junction is labeled in turn and paired with roughly stoichiometric concentrations of (a) its complete complementing strand and (b) the three remaining strands of the tetramer. Each sample is split into two aliquots, one for ligand binding and one as a control. This gives four separate lanes for each labeled strand, as indicated in the diagram. In addition, control uncut strands and a sequence lane are run.

Reaction of J1 with MPE·Fe(II) reveals a specific site of enhanced cutting by this agent, as well as several sites flanking this one that show lower reactivity relative to fully duplex controls (Guo et al., 1989). The range of chain scission due to hydroxyl radicals emanating from the bound iron of MPE·Fe(II) extends several base pairs from the position of the ring (Schultz & Dervan, 1983; Dervan, 1986). Hence, we have not been able to localize the methidium binding site precisely. The pattern of enhanced cuts is consistent with the presence of a preferred site of binding at or very near the branch point, on one of the two stacks, but not the other (see

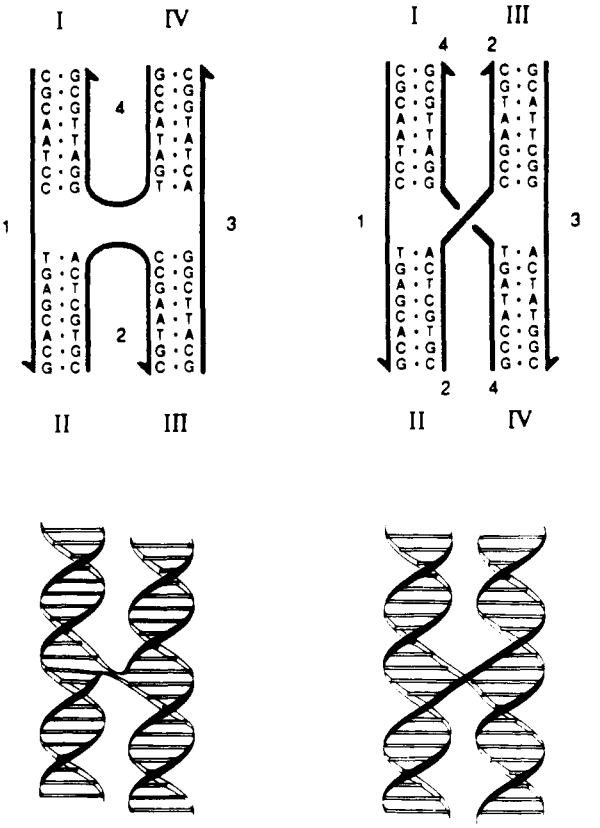

FIGURE 2: Sequence and structure of the branched junction J1. The upper panels show the junction in schematic, while the lower panels show a model of the junction based on arms of 10.5-fold B-DNA. The junction consists of four strands of DNA, indicated in the upper panels by Arabic numerals. Each strand participates in forming two double-helical arms, indicated by Roman numerals. The structural conclusion of previous work (Churchill et al., 1988) is indicated in this figure by stacking arm I on arm II and arm III on arm IV to form two helical domains. Both of the possible coplanar arrangements of these helical domains are shown, with the antiparallel arrangement on the left, and the parallel arrangement on the right.

Figure 2). In the MPE·Fe(II) experiment, the preferred site could be eliminated by competition with a second intercalator, propidium iodide (PI). This suggests that the binding site or sites involved might be favorable for intercalative binding modes in general.

In this study, we use different footprinting agents for more precise characterization of the enhanced binding site in the four-armed junction, J1 (Figure 2). The patterns of scission are determined for each of the four 16-mer strands of J1 in the tetramer and in the corresponding 16-mer duplex formed by the strand and its fully complementary 16-mer. An outline of the experimental plan is shown in Figure 1 for clarity. The probes used are EDTA·Fe(II), $(OP)_2Cu$ (I), and MPE·Fe(II) at different ratios of probe to DNA, in the presence and absence of excess propidium iodide (PI) or actinomycin D (AD). By comparison with the other probes, $(OP)_2Cu(I)$ generates greater variation in intensity of scission at different sites in duplex DNA (Drew & Travers, 1984; Spassky & Sigman, 1985; Kuwabara et al., 1986; Veal & Rill, 1989a,b) as well as greater differences between the patterns of duplex and branched DNA. Competition experiments with PI make it possible to localize the strongest binding site in J1 to the branch point itself.

Materials and Methods

Nucleic Acids. All strands used in these experiments are synthesized on an ABI 380B automated synthesizer, using

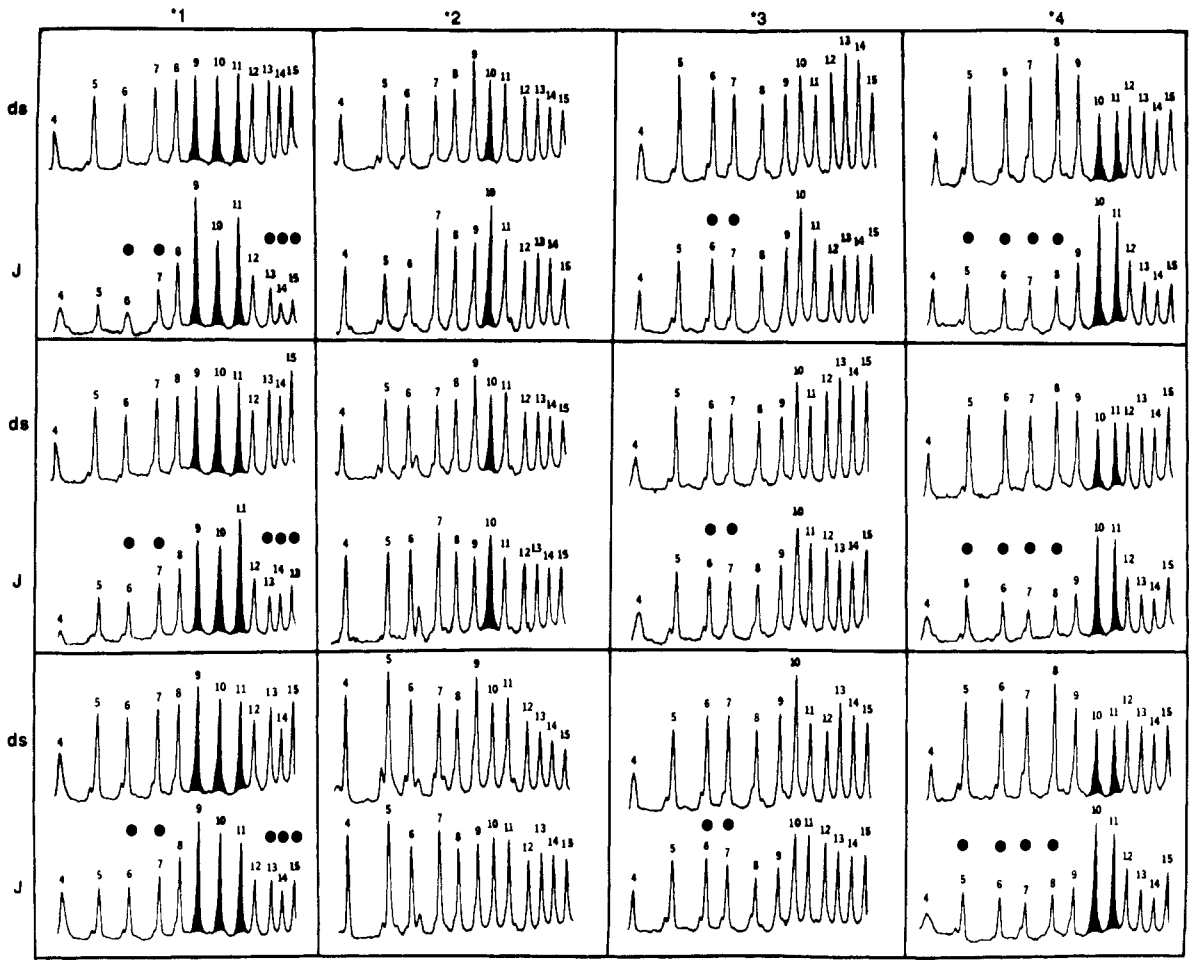

FIGURE 3: Densitometric scans of the cleavage pattern of J1 due to different concentrations of MPE·Fe(II). Each column of this figure corresponds to labeling of the indicated strand of J1. The top panel of each column corresponds to cleavage by MPE·Fe(II):J1 tetramers at a ratio of 1:16, the middle panel to a MPE·Fe(II):J1 ratio of 3:1, and the bottom panel to a MPE·Fe(II):J1 ratio of 30:1. Each panel contains two scans, one with the labeled strand in the tetramer complex (J) and one with the labeled strand in the linear duplex formed by pairing with its complementary strand (ds). The branch point lies between positions 8 and 9 on each strand. Sites of differential enhancement in this experiment are indicated as black bands in ds and J. Sites of differential protection are indicated by solid circles (●) over the corresponding bands in the J profiles. Thus, positions 9–11 on strand 1 and positions 10 and 11 on strand 4 show enhanced cleavage in the junction relative to the duplex.

standard phosphoramidite chemistry (Caruthers, 1982). Strands are purified after deprotection and removal from the synthetic columns by preparative HPLC on a Du Pont Zorbax Bio Series oligonucleotide column, using a gradient of NaCl in a solvent system containing 20% acetonitrile and 80% 0.02 M sodium phosphate. Fractions from the major peak are collected, concentrated, desalted, and lyophilized.

Phosphorylation and Strand Purification. Twenty micrograms of a specific DNA strand is dissolved in 10 μL of a solution containing 66 mM Tris-HCl, 1 mM spermidine, 10 mM $MgCl_2$, 15 mM dithiothreitol (DTT), and 0.2 mg/mL nuclease free bovine serum albumin (BSA) from BRL and mixed with 5 μL of 1.25 mM [γ-^{32}P]ATP(10 mCi/mL) and 2 units of T4 polynucleotide kinase (Boehringer) for 15 min at 37 °C. This reaction is quenched by adding 1 mM cold ATP and 1 unit of T4 polynucleotide kinase and stopped by freezing in dry ice. The mixture is rapidly heated for 5 min at 70 °C, cooled to room temperature, and loaded on a 20% denaturing polyacrylamide gel. This gel is run at 2000 V (ca. 50 V/cm) for 3 h at room temperature and exposed briefly to X-ray film (Kodak XOmat AR or Amersham Hyperfilm βmax). The band corresponding to 16-mer is cut out and soaked overnight at 37 °C in 0.5 mL of buffer (0.5 M ammonium acetate, 1 mM EDTA). This material is centrifuged for 5 min at room temperature in a microfuge and the gel re-extracted with 0.1 mL of the same buffer, precipitated twice with ethanol, and lyophilized.

MPE Cutting. Our procedure follows that of Van Dyke and Dervan (1983), with minor changes due to the short strands involved and the addition of Mg^{2+} to stabilize junctions (Seeman et al., 1985). Junctions are formed by annealing a stoichiometric mix of strands at 16 μM concentration in 50 mM Tris-HCl, pH 7.5, with 10 mM $MgCl_2$. An Eppendorf tube containing the solution is immersed in boiling water for 2 min, cooled slowly to room temperature, and finally chilled to 4 °C. Double-stranded controls are formed similarly by using a stoichiometric amount of cold strand complementary to the labeled junction strand. For cutting both branched and linear molecules, freshly prepared solutions of MPE·Fe(II) are made up in a buffer of 10 mM Tris-HCl, pH 7.4, with 50 mM NaCl, containing 1 μM Fe(II) and 2 μM MPE (Van Dyke & Dervan, 1983a). DNA (16 μM) is exposed to the reagent for 15 min at 4 °C, followed by addition of 4 mM DTT for 30 min, and the reaction is stopped by freezing on dry ice. After the solution is extracted with 1-butanol, to remove drug, and dried, the sample is taken up in formamide loading buffer, heated briefly to 90 °C, cooled, and then run on a denaturing polyacrylamide gel for 3 h at 2000 V (ca. 50 V/cm) and 40 °C. No dyes are added in these runs. The gel is dried immediately on a vacuum drying apparatus (Hoefer) and exposed at room temperature to film without an intensifier screen.

$(OP)_2Cu(I)$ Cutting. The procedure of Kuwabara et al.

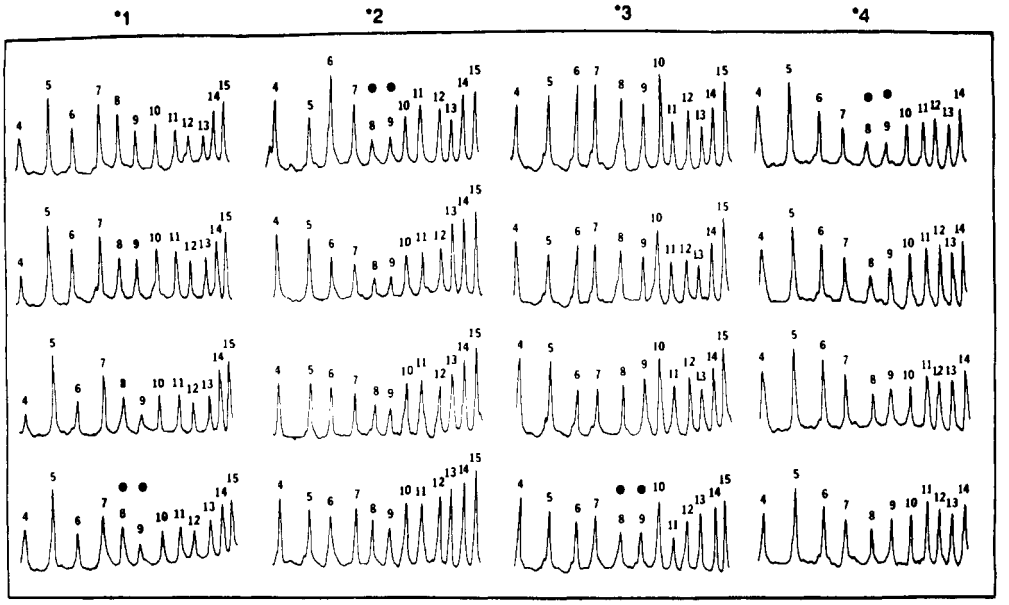

FIGURE 4: Densitometric scans of the cleavage pattern of J1 due to footprint of PI bound to J1 cutting by EDTA·Fe(II). Each column in this figure corresponds to labeling of the indicated strand of J1. Each column of scans contains four scans, from top to bottom, in which the first scan is the hydroxyl radical cleavage in the absence of PI; the second to the fourth scans are, respectively, 2.5×, 5×, and 10× molar excess of propidium to J1, following exposure to EDTA·Fe(II). (●) indicates bands inwhich the junction is protected from cleavage relative to the junction in the absence or presence of PI. Note that nearly identical protection from cleavage occurs for strands 2 and 4 at positions 8 and 9 in the absence of PI, while positions 8 and 9 show protection on strands 1 and 3, but deprotection on strands 2 and 4 in 10× molar excess of PI over J1.

(1986) is followed, except for substitution of ascorbate for mercaptopropionic acid. The reaction mixtures contain 200 μM *o*-phenanthroline (Kodak), 45 μM $CuSO_4$, and 1 mM ascorbate in addition to the buffer components described for the MPE experiments above. Reactions are allowed to proceed for 45 min at 4 °C and stopped by extraction with 1-butanol, and then the mixture is dried and loaded onto the gel in running buffer without dye.

EDTA·FE(II) Cutting. The procedure described by Churchill et al. (1988) for EDTA·Fe(II) cutting of DNA junctions is used, except that the ratio of labeled to unlabeled strands is kept nearly stoichiometric in the experiments reported here to avoid perturbing the drug/DNA ratios.

Densitometry. Autoradiograms are scanned on a Hoefer GS300 densitometer or an LKB UltroScan XL laser densitometer, Model 2222-010, without base-line corrections.

Results

Concentration Dependence of MPE·Fe(II) Scission. The experiments that initially revealed the presence of a site of enhanced cleavage by MPE·Fe(II) in the tetramer, absent in any corresponding duplexes, were carried out at a ratio of 1 MPE·Fe(II) molecule per 16 tetramers (Guo et al., 1989). At this concentration, both apparent enhancement and protection effects can be detected, relative to duplexes. It should be noted that to compare two patterns on different lanes or gels we "normalize" the two by looking for a set of adjacent bands which appear closest in profile between the two and then adjusting the intensities of the two lanes accordingly. Despite loading approximately equal numbers of counts on each lane of a gel, there is variation both in the actual volumes delivered and in the extent of cutting between different experiments. For comparison of a double-strand pattern with that of a tetramer, for example, sets of bands with similar profiles tend to occur in the vicinity of positions 3–6 or 11–14, near the ends of the arms, which are likely to yield a common pattern of cuts. By using these sites as standards, it is often possible to ascertain the presence of both protection and enhancement on a given strand. However, when our standard positions are perturbed, a change in intensity cannot be distinguished from a scaling phenomenon.

As can be seen in Figure 3, the cleavage pattern produced by MPE·Fe(II) indicates enhanced cutting at positions located on the left helical stack in J1, including **1**: 9–11, **4**: 10,11, and **2**: 10. (Our nomenclature indicates strand number in bold face, with the specific residue number counting from the 5′ end denoting the presumed site of cleavage, leaving a fragment actually one unit shorter. For example, cleavage at site **1**: 9 indicates that the probe has attacked the sugar of residue 9 in strand 1, leaving a major 5′-labeled chain fragment containing eight nucleosides with 5′-phosphate and 3′-phosphomonoester termini.) Protection at several sites distal to the branch point is observed, including **1**: 6,7,13–15, **3**: 6,7 (weak), and **4**: 5–8. Increasing the ratio of probe to DNA from this level up to 30 MPE·Fe(II) molecules per tetramer—nearly 1 MPE per base pair—results in a similar pattern of enhancement. This indicates that the site of higher affinity is occupied first and is maintained even in the presence of drug levels corresponding to saturation of normal intercalative binding [see, e.g., Mandal et al. (1980)]. However, the enhancement at **2**: 10 disappears at high ratios of drug to J1. Interestingly, the pattern of protection in strand 1 breaks down with increasing drug, while that at **4**: 5–8 persists. We see no evidence that a large relative excess of MPE·Fe(II) perturbs the junction configuration, since the strong drug binding site is maintained.

Propidium Iodide and Actinomycin D Interaction. We have noted previously that PI, a dicationic dye molecule containing the same phenanthridium ring system as MPE or ethidium bromide and which is similar in its intercalating properties [see, for example, Wilson and Lopp (1979)], appears to compete effectively with MPE·Fe(II) for the site of enhanced affinity on J1 (Guo et al., 1989). Thus, PI provides a potential model for MPE·Fe(II) in terms of recognition, but not intrinsic affinity. To find where PI binds, we exposed complexes of PI with J1 to OH radicals generated by EDTA·Fe(II) in the

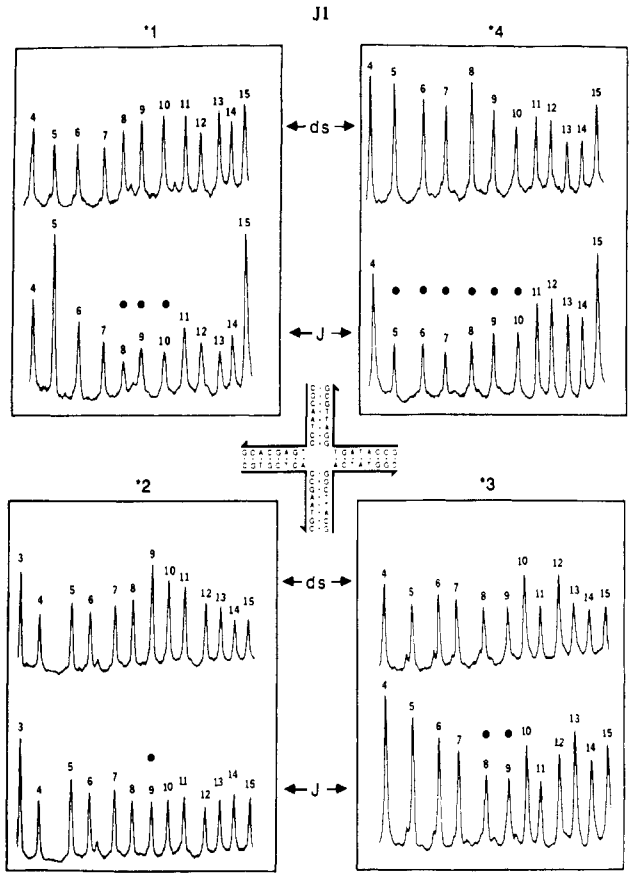

FIGURE 5: Densitometric scans of the cleavage pattern of J1 due to MPE·Fe(II) in competition with actinomycin D. Each quadrant of this figure corresponds to a given strand of J1. Each panel of scans contains two scans, one with the strand labeled in the tetrameric junction (J) and the second with the strand labeled in the corresponding linear duplex (ds). The branch point lies between positions 8 and 9 on each strand. (●) identifies bands that show differential protection in the junction relative to the duplex. Note that strong protection from cleavage is seen for strand 1 at positions 8–10 and strand 4 at positions 9 and 10. In addition, there is an elimination of the interaction on strand 2 at position 10.

presence of hydrogen peroxide (Tullius, 1988; Churchill et al., 1988). Figure 4 summarizes the results for several ratios of PI to J1. A "footprint" of PI bound to J1 emerges at sites **1**: 9 and **2**: 6, but only at relatively high ratios of drug to DNA. In contrast to MPE·Fe(II), PI at high concentrations may alter the conformational equilibrium of the junction, since the characteristic crossover isomer pattern of protection at **2**: 8,9 and **4**: 8,9 in the tetramer relative to duplexes (Churchill et al., 1988) can be seen to reverse, giving protection at **1**: 8,9 and **3**: 8,9. Since the effect is seen only at high PI:J1 ratios, it is probably not due to a single drug molecule having a preference for the reversed crossover isomer; the reversal of crossover pattern is likely to be a function of the combined interactions of several molecules with J1.

Actinomycin D (AD) consists of a planar ring system capable of intercalation into DNA, with two pentapeptide side chains (Goldberg et al., 1962). Preferential interaction of AD with GpC and related sequences in DNA has been demonstrated clearly by MPE footprinting [see Van Dyke and Dervan (1983a,b)] as well as by spectroscopic and thermodynamic methods (Muller & Crothers, 1968). The efficacy of MPE in delineating tight sites of AD binding in normal DNA implies that AD is not displaced by the probe at the concentrations used; we find the same behavior in the case of branched DNA. Figure 5 shows the MPE cutting patterns of J1 in the presence of two molecules of AD per tetramer. This footprint strongly suggests an interaction of AD in the vicinity of the site for preferential interaction of MPE and PI, probably centering on the G·C's flanking the branch site in arms I and III (Figure 2). Inhibition of cutting at **1**: 8–10, **2**: 9, **3**: 8,9, and **4**: 5–10 in J1 relative to the duplexes can be seen, together with elimination of the interaction at **2**: 10. In addition, there is an indication of a switch in intensities between sites **3**: 12 and 13 in the tetramer compared to duplex. This is an A·T sequence adjacent to three G·C's near the end of arm IV, and the effect may arise from occlusion of binding by the adjacent duplex. The protection seen in strand 3 is eliminated. Perhaps most striking is what appears to be enhancement in cutting at positions **1**: 5 and perhaps **1**: 15 as well, although this position is near the resolution limit in our gels. The former lies in an AT region, suggesting this may be an effect relayed from binding of AD at the strong site detected at **1**: 8–10. The number of sites affected suggests that more than one AD may be involved.

$(OP)_2Cu(I)$ Footprinting of J1 and Its Complexes with Intercalating Drugs. The range of diffusible OH radicals in the case of EDTA·Fe(II) and MPE extends over several base pairs (Schultz & Dervan, 1983; Van Dyke & Dervan, 1983a), and a probe with a more restricted range would be useful in localizing the interaction of different drugs with more precision. Sigman and his group have investigated the nucleolytic properties of Cu complexes with *o*-phenanthroline (Marshall et al., 1981; Pope & Sigman, 1984; Sigman, 1986; Kuwabara et al., 1986, Goyne & Sigman, 1987). The activity of this agent appears to be more localized in range than the radicals resulting from γ-irradiation (Sigman, 1986), although Williams and Goldberg (1988b) argue that a diffusible intermediate is nevertheless involved. Products of sugar ring cleavage due to abstraction of protons at both C1′ and C4′ can be detected (Kuwabara et al., 1986). Two species result from the C1′ pathway—the normally major component, the 3′-phosphomonoester, and a 3′-phospho-5-methylfuranone intermediate, which hydrolyzes slowly to yield the 3′-phosphate. The product of the C4′ reaction is a 3′-phosphoglycolate, which migrates faster than either of the products of C1′ scission.

The precise fashion in which this probe interacts with duplex DNA is not known: $(OP)_2Cu(I)$ appears to bind DNA, via the minor groove (Drew & Travers, 1984; Sigman, 1986). It is not a traditional intercalator, since a geometrically equivalent but nonscissile analogue of $(OP)_2Cu(I)$, bis(2,9-dimethyl-1,10-phenanthroline)–Cu(I), does not increase the viscosity of DNA on binding to the extent ethidium does (Graham & Sigman, 1984).

The results of cleaving the four strands of J1 in dimer and tetramer complexes are shown in Figure 6. The patterns corresponding to the duplexes alone evidently vary more in intensity than those produced by EDTA·Fe(II) or MPE. This variation has been discussed by Drew and Travers (1984), as well as by Veal and Rill (1989a,b). The latter propose that partial intercalation of $(OP)_2Cu(I)$ results in a strong sequence preference for A·T-rich units (trimers or tetramers), with inhibition due to the 2-amino group of G, at selected positions in these units. While the strong cutting at sites **1**: 5,6, **3**: 12,13, and **4**: 5–8 corresponds reasonably well to the preferred trimers pointed out by Veal and Rill (1989b), that at **2**: 5 does not. This probe appears to reflect local structural features in the minor groove of DNA, since cuts on opposite strands are staggered by three bands, the number which spans the two strands across the minor groove (Drew & Travers, 1984). Inspection of the corresponding J1 profiles shows that $(OP)_2Cu(I)$ is also more sensitive to differences between linear

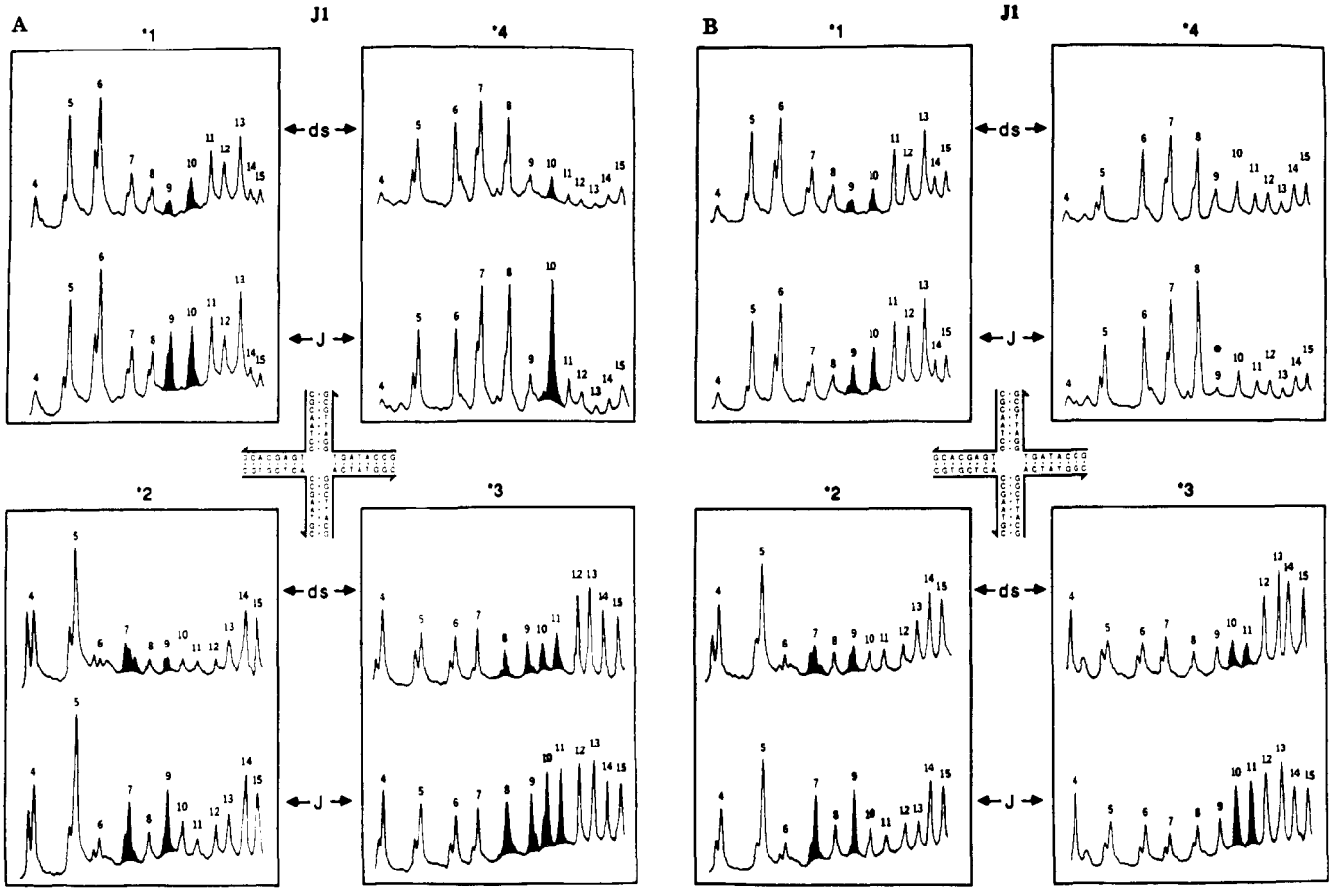

FIGURE 6: Densitometric scans of the cleavage pattern of J1 by $(OP)_2Cu(I)$ (A) and by $(OP)_2Cu(I)$ competing with propidium (B). The same conventions apply to this figure as to Figure 5. (A) As in Figure 3, sites of enhanced reactivity in the junction with respect to duplex are indicated by black bands. Thus, enhancement of cleavage is seen for strand 1 at positions 9 and 10, strand 2 at positions 7 and 9, strand 3 at position 8–11, and strand 4 at position 10. (B) Note, in particular, the disappearance of enhanced cleavage on strand 4 at position 10 and at positions 8 and 9 in strand 3. Postion 9 in strand 4 now shows protection in the junction relative to the duplex (●).

duplexes and branched molecules than the other probes we have tested. Enhanced scission at sites **1**: 9,10, **4**: 10(!), and **2**: 7,9 is evident in Figure 6A. For the first time, we discern at difference in strand 3: an enhancement at positions **3**: 8–11 relative to the duplex. Evidently, this reagent provides a sensitive probe for local differences in structure or sequence in DNA, as well as for alterations induced by protein binding (Spassky & Sigman, 1985).

Figure 6B shows the effect of PI at a ratio of two molecules to one tetramer on the $(OP)_2Cu(I)$ cutting profile of J1. The striking enhancement at **4**: 10 disappears in the presence of PI. enhancement at the opposite residue in the same arm, **1**: 8, is also lost, as is that at **1**: 9, across the branch point, and at **3**: 8,9. However, in contrast, the enhancements seen at **2**: 7,9 and **3**: 10,11 are not affected by PI binding (see below). Interestingly, site **4**: 9 is protected in the presence of PI (compare parts A and B of Figure 6). If this probe binds as a partial intercalator (Veal & Rill, 1989a,b), this might reflect exclusion of binding adjacent to the intercalated PI molecule.

In an attempt to determine the stoichiometry of PI binding, we exposed a series of complexes of J1 containing different ratios of PI to the $(OP)_2Cu(I)$ probe. The results are shown in Figure 7, in which scission is monitored on strands 3 and 4. The profiles shown reveal different dependences on the relative PI concentration at lower PI concentration, suggesting (but not proving) that the two sites reflect the effect of ligands with different affinity. Note that the titration shown is unrelated to the apparent change in crossover isomer indicated above, since that change requires much larger concentrations of PI to be detected.

In contrast to the effect of PI, AD does not eliminate the strong enhancement at **4**: 10 or that at **1**: 9 in $(OP)_2Cu(I)$ cutting (Figure 8). Thus, interaction of AD with J1 differs fundamentally from that of PI at the site of strong binding near the branch point, and in fact AD appears not to have access to the central PI site at all. It is relatively hard to discriminate the differential effect of AD on the cutting pattern of J1 by $(OP)_2Cu(I)$ relative to the free junction (Figures 6A and 8). This is true also for the EDTA·Fe(II) patterns (data not shown). The duplex profiles show stronger differences due to the binding of AD on the other hand. Exclusion of AD from the tight binding site near the branch could result from its lack of charge, hindrance by its bulky side chains, or both. However, as we have noted, MPE·Fe(II) induced scission is much more responsive to the presence of AD, possibly because it competes as an intercalator.

Discussion

Use of $(OP)_2Cu(I)$ as a Footprinting Reagent of DNA Branched Junctions. These data indicate that $(OP)_2Cu(I)$ discriminates those sites which differ in response between the duplexes and tetramer more finely than the radicals emanating from the Fe in MPE·Fe(II) in the presence of oxygen or peroxide. It is more sensitive in terms of the range of intensities corresponding to a particular sequence, as is evident from the duplex panels in Figure 6, as well as in its apparent spatial resolution. With this reagent, we can discern for the first time apparent changes in the minor groove of strand 3 imposed by the presence of the branch in the tetramer. The major site of interaction for intercalators can now be localized to the

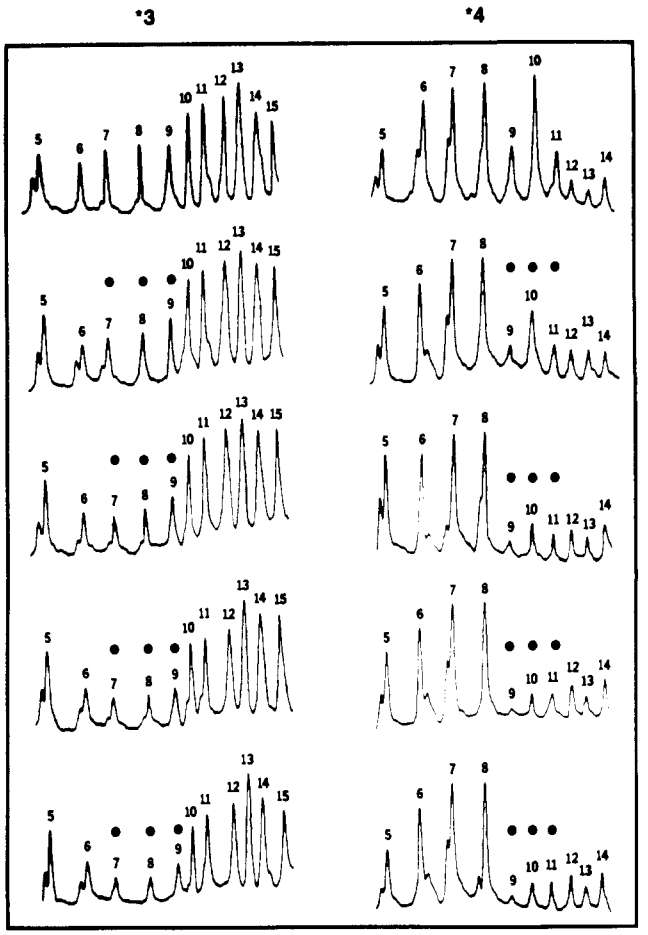

FIGURE 7: Densitometric scans of the $(OP)_2Cu(I)$-induced cleavage pattern of J1 due to the footprint of bound PI. Each column of this figure corresponds to a given strand of J1. Each column of scans contains five scans, from top to bottom, in which the first scan is the $(OP)_2Cu(I)$ cleavage; the second to the fifth scans are $^1/_8$-, $^1/_4$-, $^3/_8$-, and $^1/_2$-fold propidium to J1 cutting by $(OP)_2Cu(I)$. (●) indicates sites of protection from cutting due to PI. Note the more rapid loss of enhancement at positions 9–11 on strand 4 as the ratio of PI to J1 increases, compared to onset of protection at positions 7–9 on strand 3.

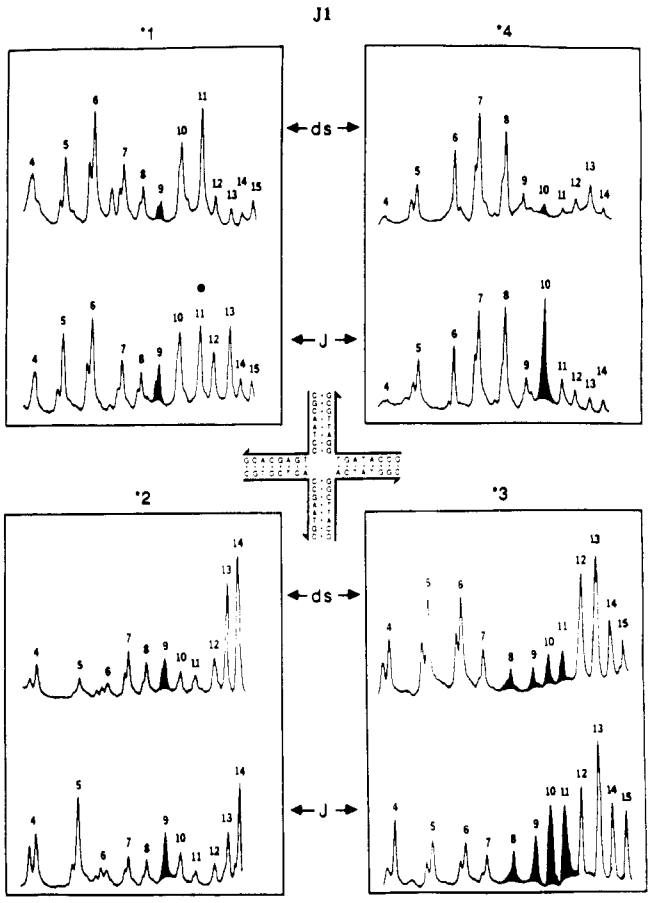

FIGURE 8: Densitometric scans of cleavage of J1 by $(OP)_2Cu(I)$ in competition with actinomycin D. The same conventions apply to this figure as to figure 5. Sites of enhanced reactivity in the junction are indicated by black bands, while sites of protection are marked by solid circles. Note that the strong enhancement on strand 4 at position 10 and that on strand 1 at position 9 in $(OP)_2Cu(I)$ cleavage still exists compared to Figure 6B.

region outlined in Figure 9B which are those for which PI eliminates the $(OP)_2Cu(I)$ enhancement: T9 of **1**,**3**: 8–9 and G10 of strand 4. Two additional sites show inhibition of cutting in the presence of PI, but no enhancement (Figure 9C). All these residues flank the branch point or are one base pair removed from it. In addition, we find evidence for the pattern of cuts on opposite strands in any of the arms of J1 staggered by three residues, as first pointed out by Drew and Travers (1984). This effect can be seen in the cleavage of both strands 1 and 4, at sites **1**: 9 and **4**: 10, for example, and suggests that the minor groove structure of the arms abutting the branch site is not deformed substantially from that in a normal double helix, a conclusion consistent with previous CD (Seeman et al., 1985; Marky et al., 1987), NMR (Wemmer et al., 1985), and protection (Churchill et al., 1988; Chen et al., 1988) data on J1.

Comparison of Branch Sites to Bulges. It is interesting to contrast these findings concerning the site of enhanced affinity for intercalators in a branched molecule with the observations of sites of enhanced affinity in duplexes containing base "bulges" (White & Draper, 1987; Williams & Goldberg, 1988a,b). The scission pattern resulting from the presence of an excess or bulged base at a specific position in a duplex is similar in some respects to what we observe for a branch site. The MPE·Fe(II) pattern of enhancement extends three residues 3′ from the actual position of the excess base (Williams & Goldberg, 1988a). However, no protected sites have been reported. Similarly, three residues 3′ to the extra base are enhanced with respect to $(OP)_2Cu(I)$ cutting, with the second base showing the strongest effect (Williams & Goldberg, 1988b). The $(OP)_2Cu(I)$ patterns associated with the particular branch we have studied show enhancement at two positions 3′ to the branch site on the two non-crossover strands, 1 and 3, but positions 5′ to the branch site between positions 8 and 9 also clearly show enhancement. In the case of this branch, flanking positions also show protection in the case of MPE·Fe(II). The patterns of cleavage of the presumptive crossover strands differ completely, as one expects, and this supports the assignments made earlier on the basis of EDTA·Fe(II)-induced cutting data (Churchill et al., 1988). One needs information on other sequences before attempting to reach general conclusions concerning the behavior of branched molecules. It would also be premature to conclude the intermediate in $(OP)_2Cu(I)$ scission is fixed or diffusible from our data, particularly in view of the problem of stoichiometry.

Structural Features of the Junction. One important conclusion from these experiments is that the dominant conformation of the immobile branched tetramer is roughly twofold symmetric, despite local differences within each of the four arms (Figure 9). That is, each arm in J1 responds distinctly in detail to the $(OP)_2Cu(I)$ probe, relative to its homologous

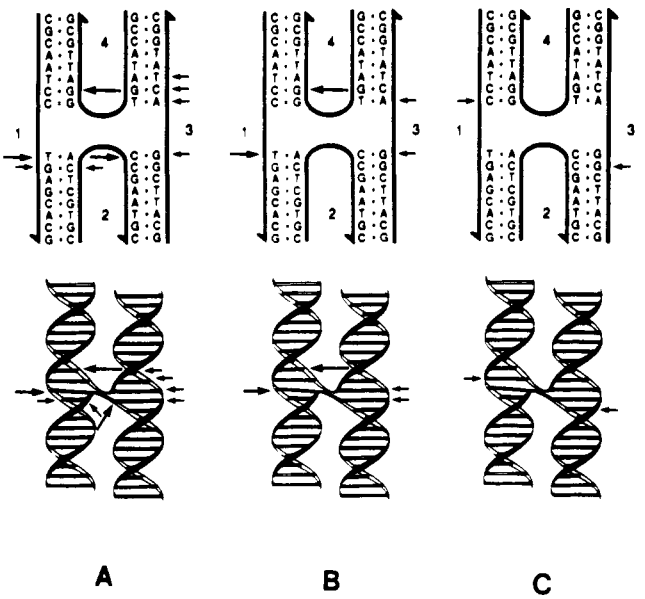

FIGURE 9: Sites of preferential drug interaction in the junction J1. Results of the scission experiments reported in this study are summarized in these panels, using the antiparallel conformer of J1 which we believe to be the predominant form in solution (Seeman et al, 1989). Sites of differential cleavage due to the interaction of J1 with $(OP)_2Cu(I)$ are indicated by arrows in panel A. The length of the arrow is a measure of the quantitative intensity of each responsive site. Panel B shows the sites from (A) for which addition of PI *blocks* the differential enhancement in $(OP)_2Cu(I)$ scission. Panel C shows in addition two sites not among those in (A) where addition of PI inhibits cutting of J1 by $(OP)_2Cu(I)$.

duplex sequence (Figure 6A). However, since cutting with $(OP)_2Cu(I)$ takes place in an excess of probe with respect to J1 (12-fold), one could imagine that this response arises from a clustering of probes along the target tetramer. To test this possibility, we repeated the experiment in Figure 6A using $^1/_{10}$ the concentration of $(OP)_2Cu(I)$, allowing the reaction to proceed 10 times longer. The results are identical with those shown in Figure 6A, arguing that this kind of clustering of adjacent drugs is not involved. The excess required may simply be due to weaker interaction of $(OP)_2Cu(I)$ with DNA than in the case of MPE·Fe(II). However, if local sequence differences outside the branch point itself are excluded by the double-strand controls in Figure 6A, then the fine structure or local environment of the minor grooves in each arm of the tetramer must be distinct from tht in the others. This conclusion is implicit in the MPE·Fe(II) cutting results of Guo et al. (1989), but not with the sensitivity now available. Nevertheless, at a cruder level, inspection of Figure 9B,C shows that the pattern of cuts differentially responsive to PI retains near twofold symmetry, as we detected first in EDTA·Fe(II)-induced scission of J1 (Churchill et al., 1988).

Crossover Reversal by PI. The observation that increased concentrations of PI can reverse the crossover isomer of J1 is of interest from a number of perspectives. As noted above, we (Chen et al., 1988) and others (Duckett et al., 1988) have shown that the sequence that flanks the branch point determines the crossover isomer. Recently, we (Mueller et al., 1988) and Duckett et al. (1988) have shown that a junction resolvase, the T4 endonuclease VII, cleaves the crossover stands in the complex. Since an odd number of crossover isomerizations are necessary to observe exchange of flanking markers (Mueller et al., 1988), a genetic consequence of this observation is that the sequence that flanks the junction may determine whether flanking marker exchange occurs. Here we note still another way in which the crossover isomer may be changed, i.e., by stressing the junction with PI. This presents a new avenue for the action of intercalative drugs in biological systems, effects on the outcome of recombination processes. Elsewhere we report that other forms of stress can also affect the crossover isomer of the junction (A. Kimball, Q. Guo, M. Lu, R. P. Cunningham, N. R. Kallenbach, N. C. Seeman, and T. D. Tullius, unpublished results). It is likely that exploration of the effects of other factors on the crossover isomer adopted by a junction will reveal still further dimensions of the recombination process.

ACKNOWLEDGMENTS

We are grateful to Dr. Warren Jelinek for use of his scanning densitometer and to Dr. Tom Tullius and his group for helpful suggestions.

Registry No. MPE·Fe(II), 83789-87-1; EDTA·Fe(II), 21393-59-9; $(OP)_2Cu(I)$, 17378-82-4; propidium iodide, 25535-16-4; actinomycin D, 50-76-0.

REFERENCES

Becker, M. M., & Wang, J. C. (1984) *Nature 309*, 682–687.
Burger, R., Berkowitz, A. R., Peisach, J., & Horwitz, S. B. (1980) *J. Biol. Chem. 255*, 11832–11838.
Caruthers, M. H. (1982) in *Chemical and Enzymatic Synthesis of Gene Fragments* (Gassen, H. G., & Lang, A., Eds.) pp 71–79, Verlag Chemie, Weinheim.
Chen, J.-H., Churchill, M. E. A., Tullius, T. D., Kallenbach, N. R., & Seeman, N. C. (1988) *Biochemistry 27*, 6032–6038.
Churchill, M. E. A., Tullius, T. D., Kallenbach, N. R., & Seeman, N. C. (1988) *Proc. Natl. Acad. Sci. U.S.A. 85*, 4653–4656.
Cooper, J. P., & Hagerman, P. J. (1987) *J. Mol. Biol. 198*, 711–719.
Dervan, P. B. (1986) *Science 232*, 464–471.
Dieckmann, S., & Lilley, D. M. J. (1987) *Nucleic Acids Res. 15*, 5765–5774.
Duckett, D. R., Murchie, A. I. H., Diekmann, S., Von Kitzing, E., Kemper, B., & Lilley, D. M. J. (1988) *Cell 55*, 79–89.
Fishel, R. (1981) Ph.D. Thesis, University of California, Irvine.
Galas, D. J., & Schmitz, A. (1973) *Nucleic Acids Res. 3*, 3157–3170.
Gilbert, W., Maxam, A., & Mirzabekov, A. (1976) in *Control of Ribosome Synthesis* (Kjelgaard, N. O., & Maaloe, O., Eds.) pp 139–148, Munksgaard, Copenhagen.
Goldberg, I. H., Rabinowitz, M., & Reich, E. (1962) *Proc. Natl. Acad. Sci. U.S.A. 48*, 2094–2101.
Goyne, T., & Sigman, D. S. (1987) *J. Am. Chem. Soc. 109*, 2846–2848.
Graham, D. R., & Sigman, D. S. (1984) *Inorg. Chem. 23*, 4188–4191.
Guo, Q., Seeman, N. C., & Kallenbach, N. R. (1989) *Biochemistry 28*, 2355–2359.
Hertzberg, R. P., & Dervan, P. B. (1982) *J. Am. Chem. Soc. 104*, 313–315.
Hertzberg, R. P., & Dervan, P. B. (1984) *Biochemistry 23*, 3934–3945.
Kallenbach, N. R., Ma, R.-I., & Seeman, N. C. (1983) *Nature 305*, 829–831.
Kuwabara, M., Yoon, C., Goyne, T., Thederahn, T., & Sigman, D. (1986) *Biochemistry 25*, 7401–7408.
Ma, R.-I., Kallenbach, N. R., Sheardy, R. D., Petrillo, M. L., & Seeman, N. C. (1986) *Nucleic Acids Res. 14*, 9745–9753.
Mandal, C., Engalander, S. W., & Kallenbach, N. R. (1980) *Biochemistry 19*, 5819–5825.

Marky, L. A., Kallenbach, N. R., McDonough, K. A., Seeman, N. C., & Breslauer, K. J. (1987) *Biopolymers 26*, 1621-1634.
Maxam, A. M., & Gilbert, W. (1977) *Proc. Natl. Acad. Sci. U.S.A. 74*, 560-564.
Mueller, J. E., Kemper, B., Cunningham, R. P., Kallenbach, N. R., & Seeman, N. C. (1988) *Proc. Natl. Acad. Sci. U.S.A. 85*, 9441-9445.
Muller, W., & Crothers, D. M. (1968) *J. Mol. Biol. 35*, 251-290.
Ogata, R., & Gilbert, W. (1977) *Proc. Natl. Acad. Sci. U.S.A. 74*, 4973-4976.
Petrillo, M. L., Newton, C. J., Cunningham, R. P., Ma, R.-I., Kallenbach, N. R., & Seeman, N. C. (1988) *Biopolymers 27*, 1337-1352.
Pope, L., & Sigman, D. S. (1984) *Proc. Natl. Acad. Sci. U.S.A. 81*, 3-7.
Schmitz, A., & Galas, D. J. (1979) *Nucleic Acids Res. 6*, 111-137.
Schultz, P. G., & Dervan, P. B. (1983) *Proc. Natl. Acad. Sci. U.S.A. 80*, 6834-6837.
Seeman, N. C. (1982) *J. Theor. Biol. 99*, 237-247.
Seeman, N. C. (1988) *J. Biomol. Struct. Dyn. 5*, 997-1004.
Seeman, N. C., & Kallenbach, N. R. (1983) *Biophys. J. 44*, 201-209.
Seeman, N. C., Maestre, M. F., Ma, R.-I., & Kallenbach, N. R. (1985) in *The Molecular Basis of Cancer* (Rein, R., Ed.) pp 99-108, Liss, New York.
Seeman, N. C., Chen, J. H., & Kallenbach, N. R. (1989) *Electrophoresis 10*, 345-354.
Siebenlist, U., Simpson, R. B., & Gilbert, W. (1980) *Cell 20*, 269-281.
Sigman, D. S. (1986) *Acc. Chem. Res. 19*, 180-186.
Spassky, A., & Sigman, D. S. (1985) *Biochemistry 24*, 8050-8056.
Tullius, T. D. (1987) *Trends Biochem. Sci. 12*, 297-300.
Tullius, T. D., & Dombroski, B. A. (1985) *Science 230*, 679-681.
Tullius, T. D., & Dombroski, B. A. (1986) *Proc. Natl. Acad. Sci. U.S.A. 83*, 5469-5473.
Van Dyke, M. W., & Dervan, P. B. (1983a) *Nucleic Acids Res. 11*, 5555-5567.
Van Dyke, M. W., & Dervan, P. B. (1983b) *Cold Spring Harbor Symp. Quant. Biol. 47*, 347-353.
Veal, J. M., & Rill, R. L. (1989a) *Biochemistry 28*, 3243-3250.
Veal, J. M., & Rill, R. L. (1989b) *Biochemistry 28*, 1822-1827.
Ward, B., Skorobogaty, A., & Dabrowiak, J. C. (1986) *Biochemistry 25*, 6875-6883.
Wemmer, D. E., Wand, A. J., Seeman, N. C., & Kallenbach, N. R. (1985) *Biochemistry 24*, 5745-5749.
White, S. A., & Draper, D. E. (1987) *Nucleic Acids Res. 15*, 4049-4064.
Williams, L. D., & Goldberg, I. H. (1988a) *Biochemistry 27*, 3004-3011.
Williams, L. D., & Goldberg, I. H. (1988b) *Nucleic Acids Res. 16*, 11607-11615.
Wilson, W. D., & Lopp, I. G. (1979) *Biopolymers 18*, 3025-3041.

1α-Hydroxylation of 24-Hydroxyvitamin D_2 Represents a Minor Physiological Pathway for the Activation of Vitamin D_2 in Mammals

Ronald L. Horst,*,‡ Nicholas J. Koszewski,§,‖ and Timothy A. Reinhardt‡

National Animal Disease Center, Agricultural Research Service, U.S. Department of Agriculture, Ames, Iowa 50010, and Department of Biochemistry and Biophysics, Iowa State University, Ames, Iowa 50011

Received June 26, 1989; Revised Manuscript Received August 29, 1989

ABSTRACT: C_{24}-Hydroxylation was evaluated as a possible activation pathway for vitamin D_2 and vitamin D_3. Routine assays showed that 24-hydroxyvitamin D_2 and 1,24-dihydroxyvitamin D_2 could be detected in rats receiving physiological doses (100 IU/day) of vitamin D_2; however, 24-hydroxyvitamin D_3 could not be detected in rats receiving similar doses of vitamin D_3. In rats, 24-hydroxyvitamin D_2 was very similar to 25-hydroxyvitamin D_2 at stimulating intestinal calcium transport and bone calcium resorption. The biological activity of 24-hydroxyvitamin D_2 was eliminated by nephrectomy, suggesting that 24-hydroxyvitamin D_2 must undergo 1α-hydroxylation to be active at physiological doses. In vivo experiments suggested that when given individually to vitamin D deficient rats, 24-hydroxyvitamin D_2, 25-hydroxyvitamin D_2, and 25-hydroxyvitamin D_3 were 1α-hydroxylated with the same efficiency. However, when presented simultaneously, 24-hydroxyvitamin D_2 was less efficiently 1α-hydroxylated than either 25-hydroxyvitamin D_3 or 25-hydroxyvitamin D_2. 1,24-Dihydroxyvitamin D_2 was also approximately 2-fold less competitive than either 1,25-dihydroxyvitamin D_2 or 1,25-dihydroxyvitamin D_3 for binding sites on the bovine thymus 1,25-dihydroxyvitamin D receptor. These results demonstrate that 24-hydroxylation followed by 1α-hydroxylation of vitamin D_2 represents a minor activation pathway for vitamin D_2 but not vitamin D_3.

Vitamin D_3 and vitamin D_2 are used for supplementation of animal and human diets in the United States. Vitamin D_3 is the form of vitamin D that is synthesized by mammals, whereas, vitamin D_2 is the major naturally occurring form of the vitamin in plants. Vitamin D_3 also occurs naturally in plants and may comprise as much as 1% of the total vitamin D in alfalfa (Horst et al., 1984a,b). Whether or not vitamin D_3 occurs naturally in other plant species is presently unknown. Nocturnal herbivores therefore would have evolved with vi-

* To whom correspondence should be addressed.
‡ U.S. Department of Agriculture.
§ Iowa State University.
‖ Present address: University of Rochester Medical Center, Rochester, NY.